Revisiting the Hammond Postulate: The Role of Reactant and Product Ionic States in Regulating Barrier Heights, Locations, and Transition State Frequencies†

Neil M. Donahue‡

Department of Chemistry and Chemical Biology, Harvard University, Cambridge, Massachusetts

Received: March 17, 2000; In Final Form: September 26, 2000

Radical−molecule reaction barriers are often the product of an avoided curve crossing between two states: the reactant ground state, which ultimately correlates with a product ionic state, and a reactant ionic state, which ultimately correlates with the product ground state. The energy, location, and loose-mode frequencies of the transition state are controlled by this interaction. The curve crossing itself is constrained by long-range Coulombic forces acting primarily on the ionic states as the reactants approach each other. The crossing height is in essence a geometric mean of the ionic surface heights; a low ionic state energy in either the reactants or the products will force a low reaction barrier. The crossing location is controlled primarily by any asymmetry in the reactant and product ionic heights, while the interaction distance of the transition state is controlled by a balance in gradients on the ground and ionic states. The frequencies related to translation of the separated reagents within the center of mass frame of reference are controlled by the same physics controlling the barrier height, as is the imaginary frequency associated with the reaction itself. This drives a tight correlation between barrier heights, transition state frequencies (and thus preexponential terms), and the imaginary frequency (and thus the tunneling term). This is demonatrated by analyzing a series of H atom transfers from a mainfold of alkanes to a mainfold of atoms. The Hammond postulate—reaction enthalpy controls transition state location—does not correspond to the mechanism controlling either barrier height or location, but rather appears to work in cases where ionization potential correlates with bond strengths.

Introduction

In several recent papers[1−3] we have described a general theory of radical−molecule reactivity on the basis of the interaction of ground and ionic states along the reaction coordinate. The theory is based on the proposition that an avoided curve crossing involving reactant and product ground and ionic states controls reaction barrier heights in many radical−molecule reactions. It draws on the work of Fukui,[4] Woodward and Hoffmann,[5] and Shaik and Pross[6,7] using orbital and far-field interactions to define the boundary conditions for a two-state avoided curve crossing problem. The unique aspect of this theory is the emphasis it places on the ionic states; they are the dominant excited states controlling the curve crossing height in many neutral reactions, not merely sources of a polar perturbation on an otherwise neutral transition state. Its unique success is to predict the evolution of barrier heights in a wide range of reactions, simultaneously describing both radical and molecule reactivity in both atom transfer and addition reactions.

The ionic state in this curve crossing is formed by transferring an electron from a high energy orbital of the electron donor (usually the molecule) to an unoccupied or singly occupied orbital of the electron acceptor (usually the radical). The state is constrained to the geometry of the ground state; the initial energy is thus the difference of the vertical ion energies $(IP-EA)_v$ when the reactants are separated. As the reactants approach, however, the energy of the ionic state decreases dramatically ($\sim e^2/r$). It rapidly drops to a lower energy than any neutral excited state, and eventually participates in the avoided curve crossing that forms the reaction barrier. Only at the curve crossing is the state occupied, and only if the crossing occurs at a great distance, in harpoon or electron jump reactions, does the reaction possess any observable ionic character.[8] Our recent papers[1−3] demonstrate that a curve-crossing model bounded by these ionic states is far more predictive than either a covalent singlet−triplet splitting model[6] or reaction enthalpy correlation.[9] In particular, the ionic curve-crossing model simultaneously predicts both radical and molecule reactivity, which the other theories cannot do.

Here we shall extend the predictive range of the theory from barrier heights to rate constants by showing how it describes the modes normal to the reaction coordinate. In particular, we will show that the loose bending modes responsible for most variation in preexponential terms are constrained by the same curve crossing, and that the frequencies of these modes are tightly coupled to the barrier heights. In the same manner, the imaginary frequency for atom transfer is also tied to the barrier height. Furthermore, the stretching mode associated with the attacking radical is insensitive to the excited-state energy but sensitive to the collisional reduced mass. With this understanding, we shall describe the evolution in both barrier heights and preexponential terms (including tunneling coefficients) for a homologous set of reactions involving a manifold of molecules reacting with a manifold of radicals.

To extend the theory we will focus on two things: first, locating the transition state, and second, describing the critical vibrational frequencies at that location. Location has two components: the distance between the reactants at the transition state, and the position of the transition state along the coordinate describing molecular distortion (ie, atom transfer). The reactant

† Part of the special issue "Harold Johnston Festschrift".

‡ Present address: Departments of Chemistry and Chemical Engineering, Carnegie Mellon University, Pittsburgh, PA, 15217. E-mail: nmd+@cmu.edu.

10.1021/jp001004t CCC: $20.00
Published on Web 11/15/2000

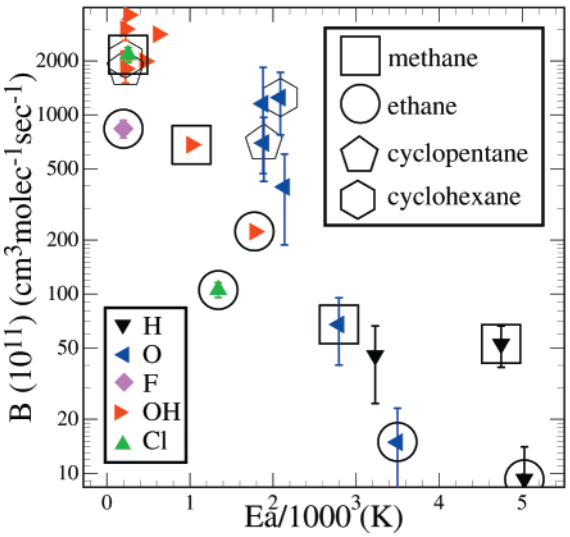

Figure 1. Preexponential terms for H atom transfers[1] vs activation energy. The preexponential terms (from a modified Arrhenius form[1] similar to one developed here) have been corrected for collisional reduced mass and the number of available H atoms.

distance is controlled by a relationship between ground and excited-state energy gradients, while the transition state position (the earliness or lateness of the transition state) is controlled by asymmetry between reactant and product excited-state energies. The physics controlling the transition state location also controls the potential energy curvature at this saddle point.

The modes critical to reactivity can all be related to translational modes of the attacking radical, though this can be obscured by a normal-mode analysis. As the excited-state energy varies from reaction to reaction, the radical stretching frequency remains constant, while the radical bending frequencies vary in concert with the barrier height. The bending frequencies control the preexponential term, while the stretching frequency, coupled with the stretch associated with the atom transfer, controls the zero-point energy change between the reactants and the transition state.

A focus of our previous work was identifying the true controlling factors in barrier height regulation amidst a sea of correlated terms. Here we have a similar goal for the preexponential. In Figure 1 we show the preexponential terms from our previous work on H atom abstractions[1] (adjusted for collisional reduced mass and number of reactive hydrogen atoms), plotted against the activation energies that were the subject of that work. Over a wide dynamic range (nearly 3 decades), there is a very tight relationship between the two, again including both variations in molecules and radicals. However, the correlation is totally empirical. We shall show here that this relationship reflects common control of both parameters. In particular, the transition state location and the loose frequencies discussed above are both controlled by the excited ionic states, but the loose frequencies (and by extension the ionic states) and not the location govern the preexponential. This is in constrast to common assumption, which focuses on the transition state location. The ubiquitous rule used to explain this location is the Hammond postulate: "If two states. . . occur consecutively during a reaction process and have nearly the same energy content, their interconversion will involve only a small reorganization of the molecular structures".[10] In other words, exothermic reactions have early transition states (resembling the reactants), and vice versa. In fact the Hammond postulate does not describe a fundamental aspect of reactivity, and its empirical success is based on the correlation of the actual controlling parameters (the excited-state energies) with reaction enthalpy for selected systems.

There is also a far more modern context for this work than the Hammond postulate. A widely accepted practice when comparing ab initio based predictions of rate constants with data is to assert that ab initio frequencies are generally quite accurate, while ab initio barriers are known to be less so. Consequently, practitioners commonly treat the barrier as an adjustable parameter while leaving the transition state frequencies fixed (see, for example, Senosiain et al. this issue[11]). The evidence for this approach is the well-established accuracy of ab initio frequency calculations on stable molecules.[12] However, there is no more evidence that this accuracy extends to transition states (in particular the loose modes that dominate the density of states) than there is evidence that the relatively accurate energies for stable molecules extend to transition states. In fact, with very few exceptions, the only data available to constrain these loose transition state frequencies are the same rate constants we use to constrain barriers. We shall argue here that there is every reason to expect the errors in transition state energies to extend to these loose modes (and to the imaginary frequency), because there is very strong evidence suggesting that barriers, loose modes, and imaginary frequencies are strongly and causally correlated.

Background

Arrhenius fitting of temperature-dependent rate data ($k = Ae^{-E_a/RT}$)[13] is ubiquitous. At least for simple reactions, the enthalpy difference between reactants and a single, well-defined transition state indeed dominates the observed temperature dependence. The preexponential in this formalism is related to the collision probability and an aggregated probability that a given collision will be properly oriented to produce the transition state. In the Arrhenius formalism, this term is temperature independent. This is, of course, not correct. The preexponential term will increase with temperature, as the system tolerates collisions off of the ideal orientation.

In transition state theory, this increased reaction probability is expressed in terms of vibrational modes at the transition state.[14] Together with partition functions associated with translation and rotation of the transition state and the reactants, partition functions for these modes describe the preexponential. (For the Hammond postulate to hold, reaction enthalpy and transition state location would have to strongly influence these modes.) Their effect on the rate constant is to cause upward curvature at high temperature; as temperature increases to the point where a given vibrational mode is activated above its zero-point energy, the partition function for that mode will grow larger than unity and consequently influence the rate constant. Though all vibrations of reactants and the transition state will contribute to the rate constant, by far the most influential are vibrational modes at the transition state that correspond to translation (and possibly rotation) of the separated reactants; the partition functions for these different types of atomic motion are qualitatively very different. These modes describe the orientation dependence of the reaction probability. Because of this, a modification of the Arrhenius formalism is often used to fit high-temperature data for application to combustion kinetics. This function ($k = B'T^n e^{-E_a/RT}$) describes the asymptotic behavior of transition state theory at high temperature.[15]

In general this vibrational activation leads to upward curvature in Arrhenius plots of rate constants; the changing partition functions for reactants and the transition state can be interpreted

as changes in the activation energy.[16] While this perspective is quite useful in the context of thermochemical representations of reactivity, it tends to obscure the separate roles of the quantum-mechanical barrier to a reaction and the vibrational modes at the transition state. Consequently, our aim is to develop a treatment in which the "activation energy" in the Boltzmann term is as closely related as possible to the actual barrier in the electronic potential.

At low temperature, when reaction barriers are high compared to the Boltzmann term, tunneling can be important (especially if the reduced mass associated with the reaction coordinate at the barrier is low).[17] Where the high temperature activation of vibrational modes can cause upward curvature in rate data at high temperatures, tunneling can cause upward curvature at low temperatures. Because of this, individuals tend to see curvature in rate data as either evidence for tunneling or evidence for vibrational activation. The truth can often lie in between.

One other, purely quantum-mechanical effect influences the rate constant; this is the zero point energy effect.[18] Because the vibrational modes of the separated reagents and the transition state are different, the total zero-point energy in each case will also be different. Because several modes are formed at the transition state and at least one is usually lost (for instance the C−H stretch in the case of H atom transfer from a hydrocarbon), the net zero-point energy effect can either raise or lower the observed barrier. For the H atom transfer example, the barrier is generally lowered. Because of this effect, there are two energy surfaces of interest:[19] the electronic potential energy surface under the Born−Oppenheimer approximation (called the Born−Oppenheimer surface), and the energy surface including zero-point energy changes (called the vibrationally adiabatic surface).

This would all be pedantic, but for one thing: we fit data, and we unavoidably attribute physical meaning to the parameters of that fitting. This is a reasonable thing to do—least-squares fitting is a form of inverse modeling, and the parameters in an inverse model are often exactly what we seek to obtain from an experiment. However, these parameters only hold meaning to the extent the model being inverted actually describes the data. For this reason, parameters in a simple Arrhenius fit are nearly meaningless; they depend on the temperature range being fit. Similarly, modified Arrhenius fits are of questionable value for more than interpolation. They are asymptotically correct at high temperature, but fail badly at low temperature, whether or not tunneling influences a given reaction.

One objective of this work is to develop a function that includes sufficient detail to be meaningful at all temperatures and to describe the influence of tunneling and zero-point energy effects. Though such a function will have too many parameters to be constrained by a single reaction, by studying many reactions all of the parameters can be meaningfully constrained. Once we achieve this objective, we can relate these parameters to real properties of the reaction—the Born−Oppenheimer barrier, the transition state frequencies, etc.—and then attempt to understand how these properties evolve from reaction to reaction.

Theory

We have shown that a wide range of atom transfer reactions can be understood in terms of a curve crossing between reactant and product ground states and purely ionic excited states.[1,2] The evolution of ground- and excited-state energies during a reaction can be described using a three-stage reaction coordinate,[1] depicted in Figure 2 for atom transfer from a molecule, RH, to a radical X. The reaction coordinate includes two distinct regions: a far-field region, (stages I and III), where long-range forces dominate and the R−X distance (r) characterizes the interaction, and a near-field region (stage II), where the R−X distance is essentially fixed and the H atom moves along the R−X axis (ρ). In the far field, the reactants are two separate species whose geometry remains undistorted by the interaction. In the near field, the reactants combine to form a single macromolecular transition complex, and distortions, including the atom transfer, dominate the nuclear motions.

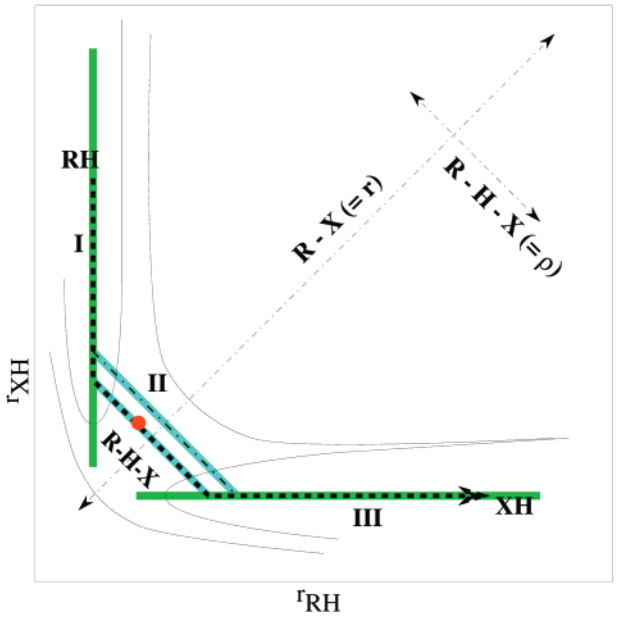

Figure 2. An approximate reaction coordinate for RH + X → R + XH, drawn on top of the ground-state surface for the R−H−X system. It develops in three stages: (I) Approach of RH and X with no geometric distortion of either species, (II) transfer of H from R to X with R−X distance constant, (III) departure of XH from R, with no relaxation.

This reaction coordinate is neither a trajectory nor a minimum energy surface but rather a mathematical construct designed to facilitate calculation of the electronic potential energy surfaces. In many cases, however, it reasonably approximates the minimum energy surface. It is particularly well suited to understanding the evolution of ionic excited states and for performing overlap calculations based on the work of Fukui.[4] Our earlier work focused on the far-field evolution of the ionic-state energies, which establishes the boundary conditions for the near-field curve-crossing problem and drives the strong correlation between measured barrier heights and ionic state energies. Here we shall consider both the height and location of the curve crossing during the atom-transfer stage, then discuss the curvature defining the critical transition-state frequencies.

State Descriptions. Following our earlier approach, we consider the ground (E^G) and ionic (E^I) states for the reaction RH + X → R + HX. These energies are functions of the R−X distance r (more precisely, they are functions of the distance between the centers of charge of the reactants). Specifically,

$$E^G = E^{G\mu} + E^{G\sigma}$$

$$E^I = E^i + E^{Iq} + E^{I\mu} + E^{I\sigma} \quad (1)$$

where E^μ represents energy due to long-range interactions (multipole moments, polarizability, etc.), E^σ represents energy related to orbital overlap (including nuclear repulsion in the near field), E^i = IP − EA is the initial ionic state energy, and

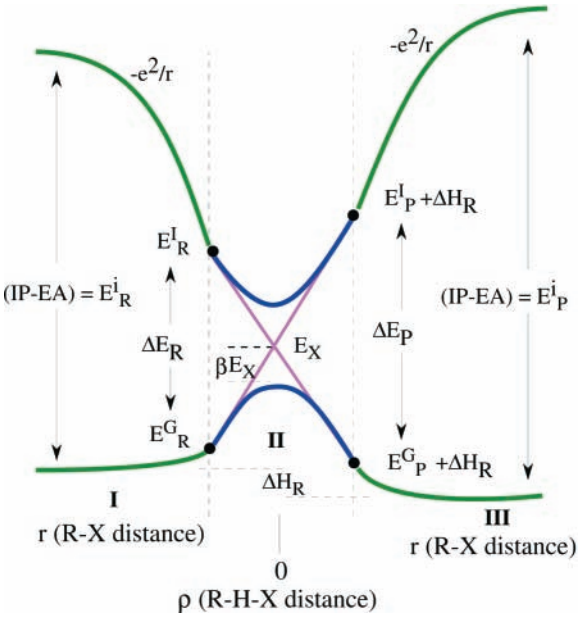

Figure 3. Evolution of ground (E^G) and ionic (E^I) energies for reactants (R) and products (P). The inner curve crossing corresponds to the atom transfer. Note that the barrier height has been exaggerated for clarity; barriers in atom transfer reactions are usually a few percent of IP-EA.

$E^{Iq} = -e^2/r$ is the Coulombic attraction between the ions. The long-range interactions are generally attractive, while the short-range interactions are repulsive. At a given r, we halt the R−X approach and allow the H atom to pass between R and X along ρ. The total distance traveled by H is $2R_x$, which is a function of r; for linear collisions, $2R_x = r - (R_{RH} + R_{HX})$, but for nonlinear collisions it is a somewhat more complicated function. During the atom transfer, the curves corresponding to the ground and ionic state energies will cross, and the reaction barrier will be found at or near the crossing point. This is shown in Figure 3. Note that $\rho = 0$ corresponds to the midpoint between R and X. We assume that the energies of the unmixed states evolve linearly over this short distance, matching the boundary conditions at either end. This simplification will affect the absolute crossing height and location, but will not in general alter conclusions about the variation of reactivity from system to system, provided that the shape of the functions remains constant.[6]

Transition State Asymmetry. We first find the location of the crossing point along the atom transfer coordinate. The crucial terms are the energy gaps between the ground and ionic states at the beginning and end of the atom transfer: $\Delta E_R = E_R^I - E_R^G$ for the reactants and $\Delta E_P = E_P^I - E_P^G$ for the products. These are all functions of r, but remain as fixed boundary conditions for a given curve-crossing problem. Normalizing to the equilibrium R−X distance, we find

$$\frac{\rho_x}{R_x} = \frac{\Delta E_R - \Delta E_P}{\Delta E_R + \Delta E_P} \tag{2}$$

Significantly, the crossing asymmetry depends only on the relative size of the gaps, and not at all on the reaction enthalpy. This is in direct opposition to the Hammond postulate. We see instead that reactions with relatively low excited-state energies in the reactants will have early barriers, while reactions with relatively low excited-state energies in the products will have late barriers. Any relationship between reaction enthalpy and transition state location is an indirect result of the strong correlation between ionization potential, singlet−triplet splittings, and bond strength in many systems.

Barrier Height. We next find the crossing height. The curve-crossing energy is

$$E_X = E_R^G + \frac{\Delta E_R(\Delta E_P + \Delta H)}{\Delta E_R + \Delta E_P} \tag{3}$$

Including the coupling term β, the barrier height is

$$E_{TS} = E_R^G + (1 - \beta)\frac{\Delta E_R(\Delta E_P + \Delta H)}{\Delta E_R + \Delta E_P} \tag{4}$$

Both the magnitude of the two gaps and the reaction enthalpy contribute to the crossing energy. However, the crossing energy is essentially the geometric mean of the gaps, meaning that a small gap on either side of the barrier will force a low crossing height. The splitting term β can be very large (of order 0.9) and is consequently a very important component of the model. Understanding the control and variation of β is a separate issue that is treated in a separate manuscript.[20]

Equation 4 is properly asymmetric, with an easily understood contribution from the reaction enthalpy. The obvious role of enthalpy is to impose a directionality on the problem; our preference is to focus on the exothermic (ethalpically preferred) direction, and to discuss barrier control in that context. Reactions proceeding against a substantial enthalpy term have an obvious and large activation term above this interesting barrier.

Though the gaps and reaction enthalpy both contribute to the crossing height, in general gap sizes (several eV) are roughly an order of magnitude larger than the enthalpy (several tenths of an eV). Furthermore, the variation in gap size from reaction to reaction is much greater than the corresponding variation in reaction enthalpy. A directly useful aspect of eq 4 is that it may be differentiated easily with respect to each term, which may in turn be related easily to measurable properties of the reactants and products. For example, have recently shown that, for nearly all of the hydrogen atom transfers referred to earlier, the most important term controlling barrier heights in eq 4 is the initial ionic state energy, IP-EA.[21] This is true over a wide range of reaction enthalpies. It is a direct consequence of the attribute noted above; because the crossing height is a geometric mean, a single small gap will force a low crossing height, and for many "normal" reactions, there is a low gap in the entrance channel corresponding to the initial ionic energy.

One might anticipate anomalous behavior from reactions with a small gap in the product channel, when the excited states and the reaction enthalpy are to some extent working in opposition. Indeed this is true; an example is the unusual kinetics of R + HBr reactions, which are discussed later in this paper.

Transition State Location. The global transition state location can be found by differentiating eq 4 with respect to r and ρ, then finding a saddle point. To isolate the factors controlling the transition state interaction distance r_x, we shall consider the symmetric problem (RH + R → R + RH), where the transition state lies at $\rho = 0$ and

$$\begin{aligned} E_x &= E^G + {}^1/_2(E^I - E^G) \\ &= {}^1/_2(E^I + E^G) \\ E_{TS} &= E_x - \beta\Delta E \end{aligned} \tag{5}$$

To find the minimum,

$$\frac{\partial E_x}{\partial r} = 0; \quad \frac{\partial E^I}{\partial r} = -\frac{\partial E^G}{\partial r} \tag{6}$$

Substituting from eq 1,

$$\frac{\partial E_{TS}}{\partial r} = \frac{\partial E^{Iq}}{\partial r} + \frac{\partial}{\partial r}(E^{I\mu} + E^{I\sigma}) + \frac{\partial}{\partial r}(E^{G\mu} + E^{G\sigma}) \tag{7}$$

which will have a minimum at

$$\frac{\partial E^{Iq}}{\partial r} + \frac{\partial}{\partial r}(E^{I\mu} + E^{I\sigma}) = -\frac{\partial}{\partial r}(E^{G\mu} + E^{G\sigma}) \tag{8}$$

This equation will only balance when the repulsive terms E^{σ} develop a significant gradient. By definition, the long-range forces will go to zero in the near field. Furthermore, the magnitude and in particular the derivatives of the overlap terms will be similar on the ground and ionic surfaces. Thus, the transition state interaction distance is defined by

$$\frac{e^2}{r^2} \simeq -2\frac{\partial E^{\sigma}}{\partial r} \tag{9}$$

When the gradient in the coulomb and exchange repulsion balances the gradient in the ionic energy, the R−X interaction distance is set and the transition state formed.

Because overlap depends strongly on distance r, eq 9 will balance at small E^{σ}; almost as soon as the ground state energy begins to climb the minimum crossing height will be established. Furthermore, the initial excited state energy IP-EA is irrelevant to the location of this saddle point; thus reactions are locked in to a strongly constrained transition state location. There is little room for variation from reaction to reaction, except for the spatial extent of the overlapping orbitals. Spatially extended systems (large radicals or easily ionized molecules) will balance eq 9 at a greater interaction distance, both because $\partial E^{\sigma}/\partial r$ will grow at larger r and because e^2/r^2 will be smaller.

Normal Modes. Having derived expressions for the transition-state location and energy, we must now consider the normal modes. These are the critical transition-state frequencies shown in Figure 4. By "normal" we mean normal to the reaction coordinate; here we shall consider the individual atomic vibrations without constructing truly normal vibrational modes. Atom−molecule reactions provide the necessary insight, so in this work we will focus our attention on those. When an atom attacks a molecule to initiate an atom-transfer, the three translational degrees of freedom of the atom are lost in favor of three vibrational modes at the transition state, while one mode of the molecule (a stretching mode associated with the atom being transferred) is lost to the reaction coordinate.

At the transition state (stage II of our reaction coordinate), the radical approach has stopped and atom transfer commenced, so this approach has transformed into a stretching mode corresponding to motion along the diagonal (R−X) in Figure 2 (ν_2 in Figure 4). The curvature of this mode is controlled by the same relationships described above in eq 7. It should not change significantly from reaction to reaction, so the frequency will only change with reduced mass (mostly varying with different radicals). For most radicals and most temperatures, this mode is inactive; however, its zero-point energy will contribute to the barrier height, leading to higher barriers for light radicals.

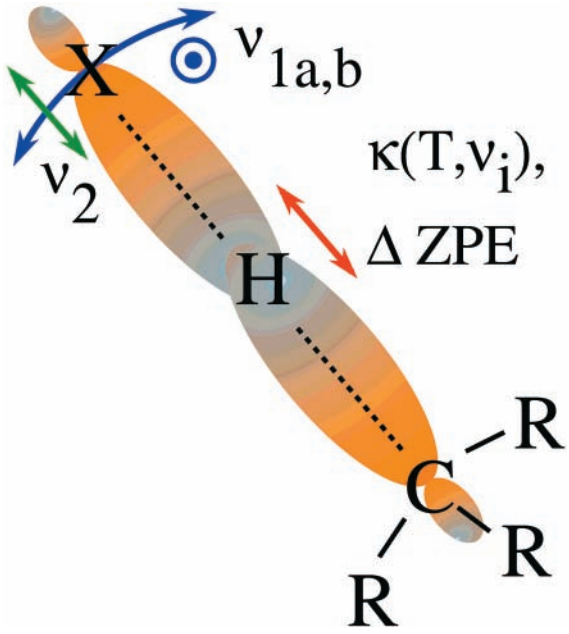

Figure 4. Normal modes influencing the rate constant, shown for radical (X) attack on a hydrocarbon. Schematic orbitals illustrate orbital overlap contributions. The imaginary mode ν_i for atom transfer controls the tunneling coefficient κ. Transverse motion of X yields two degenerate bends of low frequency that will be active at most temperatures. Longitudinal motion of X yields a higher frequency mode active only at high temperature; however, the zero-point energy associated with this mode adds to the barrier. Finally, zero-point energy lost from the imaginary mode (C−H stretch) also contributes to the barrier.

The other two modes formed from the atom translation are bends (ν_1 in Figure 4). They are nearly degenerate for linear transition states. These bends are perpendicular displacements of the attacking radical, so to first order they will not alter the excited state (ionic) energies. Curvature in the potential is generated by the breakdown of overlap in the bend, which in turn decreases the splitting term β in eq 4. We can easily see how this varies from reaction to reaction. For the normal coordinate $q_{\perp}$:

$$\frac{\partial^2 E_b}{\partial q_{\perp}^2} = \frac{\partial^2 E_R^G}{\partial q_{\perp}^2} - \beta\frac{\partial E_x^2}{\partial q_{\perp}^2} - E_x\frac{\partial^2 \beta}{\partial q_{\perp}^2} \tag{10}$$

$$\simeq E_x\frac{\partial^2 \beta}{\partial q_{\perp}^2} \tag{11}$$

Furthermore, the variation in crossing height from reaction to reaction is best described multiplicatively, i.e., $E_{xr2} = f_{r2}E_{xr1}$, so

$$\nu_{r2} = f_{r2}\nu_{r1} \tag{12}$$

In words, we expect a strong correlation between barrier heights and these loose bending frequencies. Because of neglected terms and changes in the reduced mass of this mode, the relationship between frequency and energy will not be exactly 1:1, but neither should it be 0.1:1. For a homologous series, large fractional changes in the barrier height will correspond to large fractional changes in the bending mode frequencies.

Tunneling. The imaginary frequency of the atom-transfer mode is crucial to any tunneling, which is the other source of the primary kinetic isotope effect.[17,23] The relationship between excited state energy and transverse frequency (eq 12) will also

apply to the imaginary frequency. We can approximate the influence of tunneling with a one-dimensional treatment. While this clearly neglects significant aspects of the reaction dynamics, it provides us with a heuristically useful functional form that captures the principal effects of tunneling on the thermal rate constant.

Rewriting Truhlar's one-dimensional, parabolic tunneling coefficient[17] in terms of a tunneling temperature, $T_t = \hbar\omega/(2\pi k_B)$ and a barrier temperature $T_b = E_a/k_B$, we find

$$\kappa(T) = \begin{cases} \dfrac{T_t/T}{(T_t/T) - 1}\left(\exp\left[\left(\dfrac{T_t}{T} - 1\right)\dfrac{T_b}{T_t}\right] - 1\right) & T \le T_t \\ \dfrac{\pi T_t/T}{\sin(\pi T_t/T)} - \dfrac{T_t/T}{1 - T_t/T}\exp\left[\left(\dfrac{T_t}{T} - 1\right)\dfrac{T_b}{T_t}\right] & T > T_t \end{cases} \quad (13)$$

The tunneling temperature is a characteristic temperature below which tunneling causes significant curvature in the rate constant temperature dependence. The tunneling temperature will evolve together with the barrier across a homologous series of reactions; from eq 13 we can see that this will tend to reduce the influence of tunneling as barriers are lowered.

Zero-Point Energies. Several modes contribute to zero-point energy differences between the reactants and products. One is the zero-point energy of the critical bending mode (ν_1) described above. In a homologous series, as the physics of the curve crossing simultaneously depresses the Born−Oppenheimer barrier and the bending frequency, the zero-point energy of this mode will also drop. This will amplify the effect on the observed barrier. Because of the common controlling physics, the effects will be almost impossible to separate experimentally.

Some modes associated with the atom transfer are also important. At the transition state, one stretching mode vanishes entirely (ν_i in Figure 4), and two associated bends will also be loosened. While none of these modes will be active at temperatures below ~2000 K, the reduction in zero-point energies will lower the vibrationally adiabatic barrier. For H atom transfers, this effect can be large (~2500 K), and it is a major contributor to the large primary kinetic isotope effect.[19]

Application

We can describe the temperature dependence of radical-molecule reactions with modified Arrhenius functions motivated by the above considerations. There are two reasons to do this: first, if we can write an equation that is functionally correct at both high and low temperature, we reduce the bias in our data analysis, and second, the more closely related the fit parameters are to actual physical quantities, the more useful they will be in subsequent analyses. Rather than attempting to accurately reproduce individual data points through high level calculations, we seek to understand the evolution in these fit parameters across a wide set of reactions, thereby gaining insight into the mechanisms controlling reactivity in general.

For an atom attacking a molecule, forming a linear (X−H−C) transition state, we can write a reduced transition state expression:

$$k = \frac{g(T)B\kappa(T,\nu_i)\left(10^{-10}\, S\, \mu^{-3/2}\sqrt{\dfrac{I_{TS}^3}{I_{Mol}^3}}\right)}{(1 - e^{(-1.44\nu_1)/T})^2(1 - e^{(-1.44\nu_2)/T})T^{1/2}} e^{(-E_b + \Delta E_{zp})/T} \quad (14)$$

The term $\kappa(T,\nu_i)$ is the tunneling coefficient (defined with respect to the vibrationally adiabatic barrier, $E_b + \Delta E_{zp}$), and S describes the number of identical reaction paths. The preexponential term B includes all of the vibrational partition functions we have neglected; however, all of the neglected modes will be present in both the reactant molecule and in the transition state, and in general their frequencies will be similar in each case. Thus, even if the modes are active, the partition functions should cancel. For this reason, B can not be substantially different from unity. As we shall see, this is a powerful constraint.

The electronic coefficient, $g(T)$ accounts for degeneracy at the transition state (usually the spin multiplicity of the transition state) and the electronic partition function of the radical. Consistent with current theory, we assume that only the ground electronic state at the transition state contributes to the reaction, while several low-lying electronic spin−orbit states of the radical may be important.[22] To account for the Jahn−Teller transition states in $O(^3P)$ + RH reactions we assign a spin-degeneracy of 6 to the transition state in these reactions.[22] The bottom line effect of this term is to reduce the rates for $^2P_{3/2}$ radicals (halogens) by slightly more than a factor of 2 and add a small additional temperature dependence to $O(^3P)$ reactions.

By itself, this expression is no different than any other presentation of transition state theory. Viewed in the context of what controls the terms in these expressions, however, it clearly suggests a strategy for separating these terms using a series of atom transfers from different molecules to different radicals. Also, because this expression is fundamentally experimental (in that it is used to fit data), there is no need to claim that the frequencies of these normal modes are exactly at the saddle point. The reduced transmission coefficient found in variational transition state theory is easily and naturally accommodated.

What we can now say is that ν_i, ν_1, and E_a should vary in concert. Therefore, we should be able to analyze data from a series of reactions using the above functional form to reveal this relationship. Because our objective is to analyze a series of reactions in which both the molecules and radicals are changed, we have explicitly included the change in zero point energy. This is another contribution to the barrier height that we should be able to extract from experimental data without turning to high level calculations. In particular, by paying careful attention to how primary and secondary kinetic isotope effects vary over a wide range of temperatures in an extensive reaction set, we should be able to separate the tunneling and vibrational isotope effects, thus providing experimental constraints on all of the important terms contributing to reactivity.

Results

Atom Transfer by Atoms. Now we can again consider the relationship between barrier height and the pre-exponential shown in Figure 1. In the analysis leading to that figure,[1] we held the frequencies fixed in equations similar to 14, neglected tunneling, and fit for a combined preexponential including all of the other non-exponential terms. To produce Figure 1 we removed the contribution of the reduced mass (μ) and crudely accounted for the number of reactive hydrogens as the number of most substituted hydrogens. Now we understand how the frequencies should vary, and we have collected most of the poorly constrained parameters into a single parameter (B) in eq 14 that should be close to unity. For the broad series shown in Figure 1, at least two other issues want better constraint: often multiple reaction pathways contribute to the overall rate constant, and for abstractions by OH radicals the mode associated with OH rotation or torsion about the transition state introduces uncertainty.

We have therefore reanalyzed the data for a subset of these reactions (H, O, F, and Cl + methane, ethane, cyclopentane, and cyclohexane); abstractions by atoms where there is little ambiguity as to the appropriate number of reactive pathways. These are the reactions plotted with supplemental open symbols in Figure 1. This analysis is impossible without including tunneling. The vibrational terms in eq 14 cannot go below unity, and yet without a tunneling term the data for the reaction H + methane can only be fit with the parameter B equal to ~0.05, which is unrealistically low. However, by including tunneling (eq 13), we can hold the preexpoential term at unity and obtain a reasonable imaginary frequency (−1750/cm) and radical-bend frequency (550/cm). This strongly confirms the computational results showing a significant tunneling coefficient in H atom transfers with large barriers.[23,24]

This example also serves to illustrate the limits to our ability to treat the solution to eq 14 as a strict inverse problem. Several parameters show strong covariance, and it is difficult or even impossible to fit for all of them without imposing additional constraints. In this case our main constraint is that the parameters be physically "reasonable," which is another reason for insisting that the parameters relate directly to physical properties of the reaction. Within the confines of reasonability, however, the parameters resulting from this exercise are derived results, not *a priori* guesses.

Though there is considerable freedom presented by the parameters in eq 14, the analysis of a series of reactions provides sufficient constraint, as we shall see below. In this analysis, we require a preexponential (B) near unity (within ~10%) and vary the transverse frequencies (assumed degenerate) and imaginary frequency until this condition is met. The moments of inertia are fixed, based on low level ab-initio determinations of the saddle point location, and the radical stretch frequency varies only with collisional reduced mass. The normal frequencies augment the rate constant at high temperature, when the vibrational partition function grows, while tunneling augments the rate at low temperature.

The results are shown in Figure 5. The first part (Figure 5a) shows an example fit for Cl + methane. In addition to the data, three functions are shown. The overall fit describes the data, easily reproducing the observed curvature. Below that is the same function with the tunneling coefficient set to unity; the difference between these two curves is thus the tunneling contribution. It grows from ~20% at 500 K to a factor of 10 at 200 K. This agrees well with recent computational results.[25] Below this curve is the same function with both tunneling and the vibrational partition function set to unity; the difference between these lower two curves is thus the contribution of vibrational activation at the transition state. This contribution is an almost perfect inverse of the tunneling. For this reaction the observed curvature is therefore due neither to tunneling at low temperature nor vibrational activation at high temperature but an equal mix of both.

The remaining panels in Figure 5 show the important parameters from the analysis. In Figure 5b we compare the relationship between the predicted curve crossing height and the observed barrier. The details of this calculation are identical to those presented in our earlier work;[1] the results is, if anything, more compelling. The barrier height plotted on the ordinate is now closely tied to the Born−Oppenheimer barrier height because we have now accounted for both zero-point energy changes and tunneling. The resulting correlation is considerably tighter than before. In particular, we now understand the seemingly anomalous barriers for abstraction by H atoms. The activation energy in those reactions is increased by ~500 K by the high zero-point energy of the H atom approach coordinate, as described earlier.

Figure 5c shows the relationship between the barrier heights and the imaginary frequencies for these reactions. It is very tight, as expected—there are few if any complicating factors here. Not only is the correlation tight, but both the barrier height and the imaginary frequency vary over a wide range; we are not looking at a subtle effect. This is consistent with our earlier assertion that the boundary conditions imposed by the ionic states dominate both of these terms.

The imaginary frequency derived here may or may not correspond directly to an ab initio imaginary frequency; it is a fitting result and should thus be regarded as a characteristic frequency that provides the tunneling demanded by the data and the functional form we have employed for the tunneling contribution. For example, work presented in this issue suggests that a WKB treatment carried out along the minimum energy path yields a far more accurate tunneling correction than a simple calculation based on the computed imaginary frequency.[11] Our result in no way contradicts this. We do find that this frequency evolves over the reaction series, and in this we disagree with earlier treatments,[23] which have either found or assumed a nearly constant imaginary frequency within a given class of reactions (such as H atom transfer).

Finally, Figure 5d shows the relationship between the barrier heights and the normal frequency. Again, there is a pronounced relationship, albeit with more scatter. This is consistent with our expectations; Other factors, such as the reduced mass of these bends, also contribute to the result. At one extreme (Cl + methane), the attacking radical is heavy compared to the molecular group (methyl), while at the other extreme (O + cyclohexane), the attacking radical is light. This certainly contributes to the observed spread. Furthermore, all other sources of variability, including experimental error, have been visited on this one parameter. Notwithstanding, there is a strong correlation between barrier heights and the normal frequencies; at this point all of the terms associated with the observed rate constants are explained by our simple theory.

Discussion

General Issues. This work strongly confirms our earlier conclusion that the crossing of ionic and neutral surfaces controls barrier heights in many radical-molecule reactions.[1] The excited state used in this analysis is purely ionic; we do not create a mixed state including both covalent and ionic components, which is necessary in some other systems.[3,6] Not only have we now eliminated several simplifying assumptions of that work, we have simultaneously described the evolution of all of the important parameters controlling reactivity in these reactions, not just the barrier height. In this reaction set, for both barrier height and preexponential terms, reaction enthalpy is at most a minor contributor. This contradicts received chemical wisdom. It also provides a qualitatively different understanding from the "singlet-triplet" model,[6] though these two models converge at second order. That model accommodates a reaction enthalpy signature, as singlet−triplet splittings are directly related to bond strengths, while ionic properties, particularly electron affinities, are not so related. The ionic properties enter at second order as a polar effect on the transition state, mixing a state with charge separation with the neutral first order transition state. In both models, the reactant and product energy gaps are the actual controlling factors of both barrier height and location. It is not necessary in our model for the transition state to be at all polar;

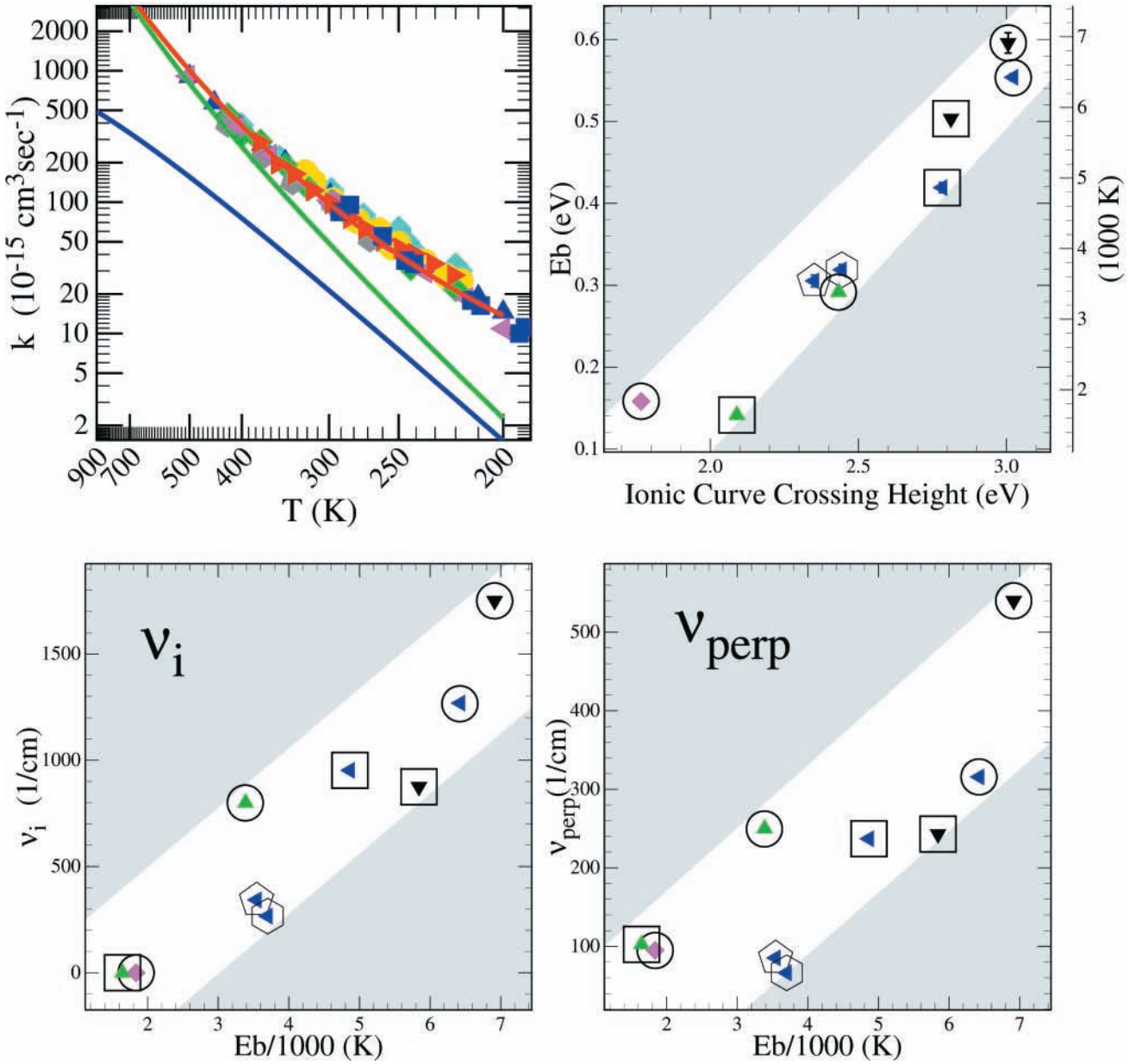

Figure 5. (a) Fit for the reaction Cl + methane. In addition to the data, three curves are shown: the overall expression for the rate constant, the rate constant with no tunneling, and the rate constant with no tunneling or vibrational activation. (b) Barrier heights vs calculated ionic curve crossing heights for a series of atoms (H, O, F, Cl) reacting with a series of alkanes (methane, ethane, cyclopentane, and cyclohexane). (c) Imaginary frequencies vs barrier heights for the same series. (d) Perpendicular (radical bend) frequencies vs barrier height for the same series. The strong covariance and tight correlations in these three plots (b, c, d) demonstrates the common controlling physics for (b) barrier heights, (c) tunneling, and (d) the preexponential.

charge separation is only generated at the transition state if excited state polarity is maintained along the reaction coordinate, which need not be so. If polarity reverses (for example, the radical on either side of the reaction coordinate is the electron acceptor), a transition state whose energy is entirely controlled by excited ionic states can show no charge separation at all.

We have recently extended this model to treat H atom additions to unsaturated hydrocarbons.[3] In that work we present a model combining covalent and ionic excited states into a mixed excited state to constrain a two state crossing problem. That analysis reveals a roughly equal contribution to addition barrier heights from both ionic and molecular triplet excited states, but shows that variation of the ionic state drives most of the variability observed in the rate constants.

Other Applications. Here we have focused on atom−molecule reactions with a single reaction pathway to isolate the critical factors driving reactivity. Treatment of OH−alkane reactions will follow; by using a similar approach, combined with data for primary kinetic isotope effects, we can accurately separate multiple reaction pathways from kinetic data and treat each pathway as a separate curve crossing. More data on both primary and secondary kinetic isotope effects for a series of radicals will substantially improve our ability to constrain these calculations.

It is also important to note that barrier height control need not be driven by the reactants; in fact, symmetry demands that either reactants or products (or both) exert control. Equation 3 reveals that a low ionic surface in either the entrance or the exit channel of the reaction will force a low barrier. Thus, there should be reactions in which the reactant ionic energy is high, and yet the barrier itself is low because of a low product ionic energy. An example is the reaction series HBr + R → Br +

RH, where the reactant ionic energy is high but the product ionic energy is very low and the barrier is correspondingly low. In this series, the reverse reaction (Br + alkane) is hindered by a large positive reaction enthalpy, despite the high electron affinity of the Br atom; however, the Br electron affinity still forces a low barrier in the enthalpically preferred direction. For instance, there is currently a significant disagreement in the experimental value of the C_2H_5 + HBr barrier,[26−28] but even the highest observed barrier is only 444 K. It is possible that the breakdown of the Hammond postulate for this reaction suggested by our theory explains the unusual temperature dependence reported in two of the studies.[26,27] The reaction has a very low barrier, a late transition state driven by a small product-channel gap, and a very strong permanent dipole in one of the reactants (HBr); consequently, the van der Waals complex in the entrance channel could play an important role in the reaction dynamics. It is possible that this complex could force the transition state energy below the reactant energy, generating a negative temperature dependence. However, confirmation of this awaits both resolution of the experimental discrepancy and more detailed theoretical treatment of the reaction.

Finally, though we have focused on understanding the preexponential, which has little to do with the transition state location, our theory does describe computed barrier locations very well. For example, we were able to reproduce ab initio barrier locations for OH attack on methane, ethane, propane, and cyclopropane using eq 2.[2] The reaction $F + H_2 \rightarrow HF + H$ is often presented as a canonical example of the Hammond postulate. The transition state is very early, and the reaction is highly exothermic (32 kcal/mol). However, the barrier location is easily understood in the context of eq 2. The reactant excited state energy much lower than the product excited state energy, and this asymmetry, not the high reactant enthalpy, produces the early transition state.

Conclusions

The difference between thermodynamics and kinetics is profound. Reaction enthalpy is a thermodynamic imperative, but it is not a kinetic motive force; it controls neither reaction barrier heights nor their location. In fact, it barely influences either. The true controlling factor of both is the excited-state splitting of reactants and products. For some covalent systems, the dominant splitting is a singlet−triplet splitting;[6] however, for many others, including many atom-transfer reactions, experimental evidence indicates that the ionic-state splittings dominate.[1] Furthermore, in general the variation of reactivity is more significant than its absolute value; in this case the influence of the ionic states is amplified by their comparatively wide dynamic range of energies.

Here we have shown how reaction barriers, tunneling, and preexponentials (dominated by a few key vibrational partition functions) vary together, driven in concert by evolving ionic excited states. We have shown that low barriers can be created by low ionic surfaces in either the entrance or the exit channel of reactions.

What have we gained? For one, we have a completely consistent description of the rate constant for atom transfers. We understand how all of the important parameters evolve in a series of reactions involving many radicals reacting with many molecules. For another, we have produced a functional form based on transition state theory including tunneling that explicitly includes all of these parameters. The combination is powerful. While the functions are under-constrained for an isolated reaction, seemingly degenerate parameters are rendered orthogonal after consideration of an appropriately constituted homologous series. Furthermore, when data are fit to these forms, the resulting parameters are theoretically meaningful; the barrier heights correspond closely to the Born−Oppenheimer barrer, while the real and imaginary frequencies correspond to the entropic constraints at the transition state. All can be directly compared to computational results. However, these functions are by no means mere regurgitations of more sophisticated theoretical computations; they are parametric forms fit to data, which reproduce the observations with great precision. Theory and experiment can now meet halfway; Arrhenius analysis produces results that can be tested against theories with the minimum necessary physics.

To return to the title of this paper, the Hammond postulate is an example of a proposition that is doubly removed from the physics truly controlling reactivity. Reaction asymmetry (the similarity of a transition state to either reactants or products) is controlled not by reaction enthalpy but by asymmetry in reactant and product ionic excited states. Furthermore, this asymmetry has little to do with observed rate constants; these are instead controlled by variations in these excited state energies from reaction to reaction, which in turn control both barrier heights and normal-mode frequencies. The Hammond postulate works, in the sense that there is often a correlation between reaction enthalpy and *A* factors, but this is essentially coincidence.

Acknowledgment. The author gratefully acknowledges the assistance of Jim Anderson, Jim Clarke, Heather Rypkema, and Jesse Kroll in this work. This work was supported by Grant ATM-9414843 from the National Science Foundation.

References and Notes

(1) Donahue, N. M.; Clarke, J. S.; Anderson, J. G. *J. Phys. Chem.* **1998**, *102*, 3923.
(2) Clarke, J. S.; Kroll, J. H.; Donahue, N. M.; Anderson, J. G. *J. Phys. Chem.* **1998**, *102*, 9847.
(3) Clarke, J. S.; Rypkema, H. A.; Kroll, J. H.; Donahue, N. M.; Anderson, J. G. *J. Phys. Chem.* **2000**, *104*, 5254.
(4) Fukui, K.; Fujimoto, H. *Bull. Chem. Soc. Jpn.* **1968**, *41*, 1989.
(5) Woodward, R. B.; Hoffman, R. *The Conservation of Orbital Symmetry*; Verlag Chemie: Weinheim, Germany, 1970.
(6) Shaik, S. S.; Hiberty, P. C. *Adv. Quantum Chem.* **1995**, *26*, 99.
(7) Pross, A.; Yamataka, H.; Nagase, S. *J. Phys. Org. Chem.* **1991**, *4*, 135.
(8) Herschbach, D. R. *Adv. Chem. Phys.* **1966**, *10*, 319.
(9) Marcus, R. A. *J. Phys. Chem.* **1968**, *72*, 891.
(10) Hammond, G. S. *J. Am. Chem. Soc.* **1955**, *77*, 334.
(11) Senosiain, J. P.; Musgrave, C. B.; Golden, D. M. *J. Phys. Chem. A* **2001**, *105*, xxxx.
(12) Scott, A.; Radom, L. *J. Phys. Chem.* **1996**, *100*, 16502.
(13) Arrhenius, S. *Z. Phys. Chem.* **1889**, *4*, 226.
(14) Eyring, H. *J. Chem. Phys.* **1935**, *3*, 107.
(15) Atkinson, R. *J. Phys. Chem. Ref. Data, Monogr. 2* **1994.**
(16) Zavitsas, A. A. *J. Am. Chem. Soc.* **1998**, *120*, 6578.
(17) Skodje, R. T.; Truhlar, D. G. *J. Phys. Chem.* **1991**, *85*, 624.
(18) Marcus, R. A.; Rice, O. K. *J. Phys. Colloid Chem.* **1951**, *55*, 894.
(19) Hu, W. P.; Rossi, I.; Corchado, J. C.; Truhlar, D. G. *J. Phys. Chem.* **1997**, *101*, 6911.
(20) Rypkema, H. A.; Donahue, N. M.; Anderson, J. G. *J. Phys. Chem. A* **2001**, *105*, xxxx.
(21) Clarke, J. S.; Rypkema, H. A.; Kroll, J. H.; Donahue, N. M.; Anderson, J. G. *J. Phys. Chem. A* **2000**, *104*, 4458.
(22) Cohen, N.; Westberg, K. R. *Int. J. Chem. Kinet.* **1986**, *18*, 99.
(23) Rodgers, A. S. *Int. J. Chem. Kinet.* **1993**, *25*, 41.
(24) Corchado, J. C.; Espinosa-García, J.; Roberto-Neto, O.; Chuang, Y.-Y.; Truhlar, D. G. *J. Phys. Chem. A* **1998**, *102*, 4899.
(25) Roberto-Neto, O.; Coitino, E. L.; Truhlar, D. G. *J. Phys. Chem. A* **1998**, *102*, 4568.
(26) Seakins, P. W.; Pilling, M. J.; Niiranen, J. T.; Gutman, D.; Kransnoperov, L. N. *J. Phys. Chem.* **1992**, *96*, 9847.
(27) Nicovich, J. M.; C. A. van Dijk, Kreutter, K. D.; Wine, P. J. *J. Phys. Chem.* **1991**, *95*, 9890.
(28) Dobis, O.; Benson, S. W. *J. Phys. Chem.* **1997**, *101*, 6030.